Journal of Sound and Vibration (2001) **248**(2), 195–214
doi:10.1006/jsvi.2000.3506, available online at http://www.idealibrary.com on IDEAL®

HYGROTHERMAL EFFECTS ON THE DYNAMIC BEHAVIOR OF MULTIPLE DELAMINATED COMPOSITE PLATES AND SHELLS

P. K. Parhi

Department of Aerospace Engineering, Indian Institute of Technology, Kharagpur 721302, *India*

S. K. Bhattacharyya

Department of Civil Engineering, Indian Institute of Technology, Kharagpur 721302, *India*

AND

P. K. Sinha

Department of Aerospace Engineering, Indian Institute of Technology, Kharagpur 721302, *India. E-mail: pksinha@aero.iitkgp.ernet.in*

(*Received* 23 *March* 2000, *and in final form* 4 *September* 2000)

A quadratic isoparametric finite element formulation based on the first order shear deformation theory is presented for the free vibration and transient response analysis of multiple delaminated doubly curved composite shells subjected to a hygrothermal environment. A simple multiple delamination model developed by the authors earlier is employed to take care of any number/size of delamination located anywhere in the laminate. The analysis takes into account the lamina material properties at elevated moisture concentration and temperature. Newmark's direct integration scheme is used to solve the dynamic equation of equilibrium at every timestep during the transient analysis. Several numerical examples are considered and the results are compared with those available in the literature. The results show a reduction in the fundamental frequency with an increase in the percentage of uniform moisture content as well as temperature for simply supported antisymmetric crossply and angleply laminates for any size of delamination considered. The central dynamic displacements and the stresses at the center of laminates are observed to increase due to the effect of moisture/temperature subjected to the suddenly applied uniform pulse loading

1. INTRODUCTION

Composite materials are being increasingly used in aerospace, civil, naval and other high-performance engineering applications due to their light weight, high-specific strength and stiffness, excellent thermal characteristics, ease in fabrication and other significant attributes. Structures used in the above fields are more often exposed to high temperature as well as moisture. The varying environmental conditions due to moisture absorption and temperature seem to have an adverse effect on the stiffness and strength of the structural composites. As, the matrix is more susceptible to the hygrothermal condition than the fiber, the deformation is observed to be more in the transverse direction of the composite. The rise in moisture and temperature reduces the elastic moduli of the material and induces internal

0022-460X/01/470195 + 20 $35.00/0

initial stresses, which may affect the stability as well as the safety of the structures. Hence, the changes in dynamic characteristics due to the hygrothermal effect seem to be an important consideration in composite analysis and design, which are of practical interest.

Delamination is one of the most frequently encountered types of damages in composite structures. It is in the form of separation of two adjacent layers resulting from high interlaminar stresses. Laminates are prone to delamination during fabrication, assembly, transportation or during normal use. Common types of delaminations are due to high- and low-energy impact, exposure to a hygrothermal environment, abrasions, high stress concentrations at geometric or material discontinuities and interlaminar shear failure. Delamination is usually induced at relatively low load levels, well before the full load capacity of the fibers is developed. In many cases, it may be in invisible form being a reliability concern for aircraft, aerospace and other advanced structural systems. As the presence of delamination in composite laminates may adversely affect the safety and durability of structures, a comprehensive understanding of the delamination behavior is of fundamental importance in the assessment of structural performance of laminated composites.

The effect of environment on the free vibration of laminated plates was studied by Whitney and Ashton [1]. They used the Ritz method to analyze symmetric laminates and equilibrium equations of motion based on the classical laminated plate theory for finding the natural frequencies of simply supported plates subjected to moisture and temperature effect. Dhanaraj and Palaninathan [2] used the semi-loof shell element to study the free vibration characteristics of composite laminates under initial stress, due to temperature. They presented the results showing the effect of temperature on the natural frequencies of antisymmetric laminates. Sai Ram and Sinha [3] investigated the effects of moisture and temperature on the free vibration of laminated composite plates using the finite element method. Results were presented showing the reduction in the natural frequency with the increase in uniform moisture concentration and temperature for different laminates with varying boundary conditions. Research study on the dynamic behavior of delaminated composites is also very scarce in the open literature. Tracy and Pardoen [4], Paolozzi and Peroni [5], and Shen and Grady [6] investigated the effect of single delamination on the free vibration of composite beams using the "four region approach". Tenek *et al.* [7] used a similar approach for the simply supported composite plates. Krawczuk *et al.* [8] studied the influence of fatigue cracks and delaminations on the dynamic characteristics of laminated composite plates. Parhi *et al.* [9–12] investigated the free vibration, transient response as well as impact and ply failure analysis of composite laminates with multiple delaminations placed at any arbitrary location of the laminate.

There is hardly any research paper available in the open literature dealing with the study of dynamic behavior of delaminated composites subjected to the hygrothermal environment. The present work is aimed at developing a finite element method for free vibration and transient response analysis of multiple delaminated composite plates and shells subjected to uniform moisture content and temperature separately. Numerical results are generated to analyze the variation of fundamental frequency of single and multiple delaminated simply supported plates and shells with varying moisture contents as well as temperatures. The effects of curvature, lamination scheme, etc., are studied for different cases. The transient response of such laminates under uniform pulse loading is also investigated for several varying delamination sizes, exposed to moisture/temperature condition. The analysis incorporates the transverse shear deformation and rotary inertia into account according to the Yang–Noris–Stavsky theory, which extends the Mindlin theory to laminated composite plates. A simple multiple delamination model is developed which can take care of any number of delaminations located anywhere along the thickness.

Free vibration results are checked with those existing in the literature.

2. FINITE ELEMENT STRUCTURAL ANALYSIS

A laminated doubly curved shell panel of length a, width b and thickness h consisting of n arbitrary number of anisotropic layers is considered as shown in Figure 1. The layer details of the laminate are shown in Figure 2. The displacement field is related to midplane displacements and rotations as

$$u(x, y, z, t) = u^0(x, y, t) + z\theta_x(x, y, t),$$

$$v(x, y, z, t) = v^0(x, y, t) + z\theta_y(x, y, t),$$

$$w(x, y, z, t) = w^0(x, y, t), \tag{1}$$

where u, v and w are displacements in x, y and z directions, respectively, and the superscript (^{0}) corresponds to the midplane values. Here, θ_x and θ_y denote the rotations of the cross-sections perpendicular to the y- and x-axis respectively. Using Sanders' first approximation theory for thin shells, the generalized strains in terms of midplane strains and curvatures are expressed as

$$\{\varepsilon_{xx}, \varepsilon_{yy}, \gamma_{xy}, \gamma_{xz}, \gamma_{yz}\}^{\mathrm{T}} = \{\varepsilon^0_{xx}, \varepsilon^0_{yy}, \gamma^0_{xy}, \gamma^0_{xz}, \gamma^0_{yz}\}^{\mathrm{T}} + z\{k_{xx}, k_{yy}, k_{xy}, k_{xz}, k_{yz}\}^{\mathrm{T}}, \tag{2}$$

where

$$\begin{Bmatrix} \varepsilon^0_{xx} \\ \varepsilon^0_{yy} \\ \gamma^0_{xy} \\ \gamma^0_{xz} \\ \gamma^0_{yz} \end{Bmatrix} = \begin{Bmatrix} \dfrac{\partial u^0}{\partial x} + \dfrac{w}{R_x} \\ \dfrac{\partial v^0}{\partial y} + \dfrac{w}{R_y} \\ \dfrac{\partial u^0}{\partial y} + \dfrac{\partial v^0}{\partial x} + \dfrac{2w}{R_{xy}} \\ \theta_x + \dfrac{\partial w}{\partial x} \\ \theta_y + \dfrac{\partial w}{\partial y} \end{Bmatrix} \quad \text{and} \quad \begin{Bmatrix} k_{xx} \\ k_{yy} \\ k_{xy} \\ k_{xz} \\ k_{yz} \end{Bmatrix} = \begin{Bmatrix} \dfrac{\partial \theta_x}{\partial x} \\ \dfrac{\partial \theta_y}{\partial y} \\ \dfrac{\partial \theta_x}{\partial y} + \dfrac{\partial \theta_y}{\partial x} \\ 0 \\ 0 \end{Bmatrix} \tag{3}$$

and R_x, R_y, and R_{xy} are the three radii of curvature of the shell element. All the dynamic equations of equilibrium reduce to that for the plate, when the values of R_x, R_y, and R_{xy} become ∞. The five degrees of freedom considered at each node of the element are u^0, v^0, w, θ_x and θ_y. By using the eight-noded element shape functions, the element displacements are expressed in terms of their nodal values given by

$$u^0 = \sum_{i=1}^{8} N_i u_i^0, \quad v^0 = \sum_{i=1}^{8} N_i v_i^0, \quad w = \sum_{i=1}^{8} N_i w_i, \quad \theta_x = \sum_{i=1}^{8} N_i \theta_{xi}, \quad \theta_y = \sum_{i=1}^{8} N_i \theta_{yi}, \tag{4}$$

where N_i's are the shape functions used to interpolate the generalized displacements, u_i^0, v_i^0, w_i, θ_{xi} and θ_{yi} at node i within an element.

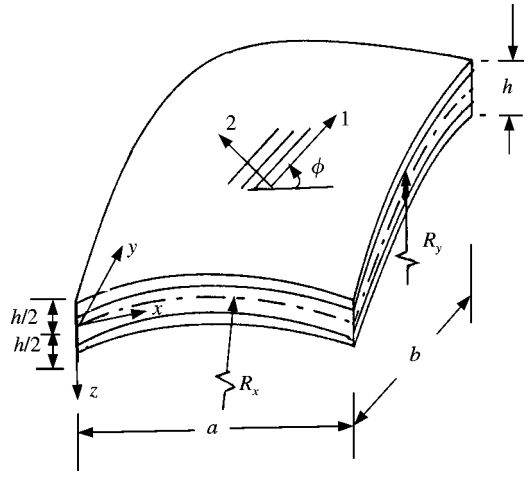

Figure 1. Laminated doubly curved composite shell axes.

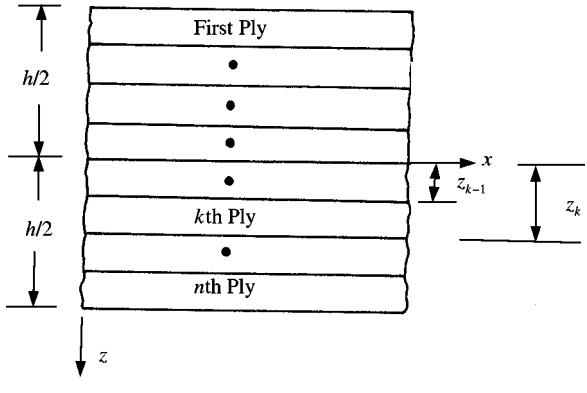

Figure 2. Layer details of the shell panel.

The stress resultants are related to the midplane strains and curvatures for a general laminated shell element as

$$\begin{Bmatrix} N_x \\ N_y \\ N_{xy} \\ M_x \\ M_y \\ M_{xy} \\ Q_y \\ Q_x \end{Bmatrix} = \begin{bmatrix} A_{11} & A_{12} & A_{16} & B_{11} & B_{12} & B_{16} & 0 & 0 \\ A_{12} & A_{22} & A_{26} & B_{12} & B_{22} & B_{26} & 0 & 0 \\ A_{16} & A_{26} & A_{66} & B_{16} & B_{26} & B_{66} & 0 & 0 \\ B_{11} & B_{12} & B_{16} & D_{11} & D_{12} & D_{16} & 0 & 0 \\ B_{12} & B_{22} & B_{26} & D_{12} & D_{22} & D_{26} & 0 & 0 \\ B_{16} & B_{26} & B_{66} & D_{16} & D_{26} & D_{66} & 0 & 0 \\ 0 & 0 & 0 & 0 & 0 & 0 & A_{44} & A_{45} \\ 0 & 0 & 0 & 0 & 0 & 0 & A_{45} & A_{55} \end{bmatrix} \begin{Bmatrix} \varepsilon^0_{xx} \\ \varepsilon^0_{yy} \\ \gamma^0_{xy} \\ k_x \\ k_y \\ k_{xy} \\ \gamma_{yz} \\ \gamma_{xz} \end{Bmatrix} - \begin{Bmatrix} N^N_x \\ N^N_y \\ N^N_{xy} \\ M^N_x \\ M^N_y \\ M^N_{xy} \\ 0 \\ 0 \end{Bmatrix}, \quad (5)$$

where N_x, N_y and N_{xy} are in-plane stress resultants, M_x, M_y and M_{xy} are moment resultants and Q_x, Q_y are transverse shear stress resultants. The terms with superscript $(^N)$ represent the corresponding non-mechanical inplane stress and moment resultants due to moisture and

temperature. The extensional, bending–stretching and bending stiffnesses of the laminate are expressed in the usual form as

$$(A_{ij},\, B_{ij},\, D_{ij}) = \sum_{k=1}^{n} \int_{Z_{k-1}}^{Z_k} (\bar{Q}_{ij})_k (1, z, z^2)\, \mathrm{d}z, \quad i,j = 1,2,6. \tag{6}$$

Similarly, the shear stiffness is expressed as

$$(A_{ij}) = \sum_{k=1}^{n} \int_{Z_{k-1}}^{Z_k} \alpha (\bar{Q}_{ij})_k \, \mathrm{d}z, \quad i, j = 4{,}5. \tag{7}$$

α, the shear correction factor which is derived from the Timoshenko beam concept by applying the energy principle is assumed as 5/6. It accounts for the non-uniform distribution of transverse shear strain across the thickness of the laminate.

$(\bar{Q}_{ij})_k$ in equations (6) and (7) are the off-axis stiffness values defined as

$$(\bar{Q}_{ij})_k = \begin{bmatrix} m^2 & n^2 & -2mn \\ n^2 & m^2 & 2mn \\ mn & -mn & m^2 - n^2 \end{bmatrix} (Q_{ij})_k \begin{bmatrix} m^2 & n^2 & mn \\ n^2 & m^2 & -mn \\ -2mn & 2mn & m^2 - n^2 \end{bmatrix}, \quad i, j = 1,2,6,$$

$$(\bar{Q}_{ij})_k = \begin{bmatrix} m & -n \\ n & m \end{bmatrix} (Q_{ij})_k \begin{bmatrix} m & n \\ -n & m \end{bmatrix}, \quad i, j = 4,5, \tag{8}$$

where $(Q_{ij})_k$ are the on-axis stiffness coefficients in the material direction given by

$$(Q_{ij})_k = \begin{bmatrix} Q_{11} & Q_{12} & 0 \\ Q_{12} & Q_{22} & 0 \\ 0 & 0 & Q_{66} \end{bmatrix}, \quad i, j = 1,2,6 \quad \text{and} \quad (Q_{ij})_k = \begin{bmatrix} Q_{44} & 0 \\ 0 & Q_{55} \end{bmatrix}, \quad i, j = 4,5.$$

$(Q_{ij})_k$ are calculated in the conventional manner from the values of elastic and shear moduli and the Poisson ratio values.

The non-mechanical in-plane stress and moment resultants are given by

$$\{N_x^N,\, N_y^N,\, N_{xy}^N\}^{\mathrm{T}} = \sum_{k=1}^{n} \int_{Z_{k-1}}^{Z_k} (\bar{Q}_{ij})_k \{e\}_k \, \mathrm{d}z,$$

$$\{M_x^N,\, M_y^N,\, M_{xy}^N\}^{\mathrm{T}} = \sum_{k=1}^{n} \int_{Z_{k-1}}^{Z_k} (\bar{Q}_{ij}) \{e\}_k \, z \, \mathrm{d}z, \quad i, j = 1,2,6. \tag{9}$$

Here $\{e\}_k = \{e_x \;\; e_y \;\; e_{xy}\}_k^{\mathrm{T}}$ are the non-mechanical strains of the kth lamina, oriented at an arbitrary angle θ_k, expressed as

$$\begin{Bmatrix} e_x \\ e_y \\ e_{xy} \end{Bmatrix}_k = \begin{bmatrix} m^2 & n^2 \\ n^2 & m^2 \\ -2mn & 2mm \end{bmatrix} \begin{Bmatrix} \beta_1 \\ \beta_2 \end{Bmatrix} (C - C_0) + \begin{bmatrix} m^2 & n^2 \\ n^2 & m^2 \\ -2mn & 2mm \end{bmatrix} \begin{Bmatrix} \alpha_1 \\ \alpha_2 \end{Bmatrix} (T - T_0), \tag{10}$$

where $m = \cos\theta_k$ and $n = \sin\theta_k$. β_1, β_2 are the moisture coefficients of a lamina and α_1, α_2 are the thermal coefficients. C_0 and T_0 are the reference moisture content and temperature, respectively, and C and T are the elevated moisture concentration and temperature respectively. In the present analysis, C_0 and T_0 are assumed as 0 and 300 K respectively.

The element stiffness matrix, $[K_e]$ is given by

$$[K_e] = \int_{-1}^{1}\int_{-1}^{1} [B]^{\mathrm{T}}[D][B]\, J\, \mathrm{d}\xi\, \mathrm{d}\eta, \tag{11}$$

where $[B]$ is the strain–displacement matrix, $[D]$, the elasticity matrix and J is the Jacobian. Full integration (3×3) is used for bending stiffness, whereas reduced integration (2×2) is employed to evaluate transverse stiffness of the elements. A 2-point integration eliminates the shear locking in case of thin plates.

Similarly, the consistent element mass matrix $[M_e]$ is expressed as

$$[M_e] = \int_{-1}^{1}\int_{-1}^{1} [N]^{\mathrm{T}}[\rho]\,[N] J\, \mathrm{d}\xi\, \mathrm{d}\eta \tag{12}$$

with $[N]$, the shape function matrix and $[\rho]$, the inertia matrix.

The element load vector, $\{F_e\}$ is presented by

$$[F_e] = \int_{-1}^{1}\int_{-1}^{1} [N]^{\mathrm{T}}\{q\}\, J\, \mathrm{d}\xi\, \mathrm{d}\eta, \tag{13}$$

where $\{q\}$ is the intensity of external transverse uniform loading.

The element load vector due to hygrothermal effects, $\{P_e^N\}$ is given by

$$[P_e^N] = \int_{-1}^{1}\int_{-1}^{1} [B]^{\mathrm{T}}\{F^N\}\, J\, \mathrm{d}\xi\, \mathrm{d}\eta, \tag{14}$$

where $\{F^N\} = \{N_x^N\ N_y^N\ N_{xy}^N\ M_x^N\ M_y^N\ M_{xy}^N\ 0\ 0\}^{\mathrm{T}}$, as mentioned earlier in equation (9).

As calculating shear stiffness, a 2-point integration is employed to find out element mass matrix and element force vector.

2.1. ELEMENT INITIAL STRESS STIFFNESS MATRIX

The linear strains are defined as

$$\varepsilon_{xx} = u_{,x} + w/R_x, \quad \varepsilon_{yy} = v_{,y} + w/R_y, \quad \gamma_{xy} = u_{,y} + v_{,x},$$
$$\gamma_{xz} = u_{,z} + w_{,x} - u/R_x, \quad \gamma_{yz} = v_{,z} + w_{,y} - v/R_y.$$

Assuming that w does not vary with z, the non-linear strains of the shell are expressed as [13, 14]

$$\begin{aligned}
\varepsilon_{xnl} &= [(u_{,x} + w/R_x)^2 + v_{,x}^2 + (w_{,x} - u/R_x)^2]/2,\\
\varepsilon_{ynl} &= [(u_{,y}^2 + (v_{,y} + w/R_y)^2 + (w_{,y} - v/R_y)^2]/2,\\
\gamma_{xynl} &= [(u_{,x} + w/R_x)u_{,y} + v_{,x}(v_{,y} + w/R_y) + (w_{,x} - u/R_x)(w_{,y} - v/R_y)],\\
\gamma_{xznl} &= [(u_{,x} + w/R_x)u_{,z} + v_{,x}v_{,z} + w_{,z}(w_{,x} - u/R_x)],\\
\gamma_{yznl} &= [u_{,y}u_{,z} + (v_{,y} + w/R_y)v_{,z} + w_{,z}(w_{,y} - y/R_y)].
\end{aligned} \tag{15}$$

Putting $u = u^0 + z\theta_x$ and $v = v^0 + z\theta_y$ into equation (15), the non-linear strains are modified. The above strains are expressed in matrix form as

$\{\varepsilon_{nl}\} = \{\varepsilon_{xnl}\ \varepsilon_{ynl}\ \gamma_{xynl}\ \gamma_{xznl}\ \gamma_{yznl}\}^{\mathrm{T}} = [R]\,\{d\}/2$, where $[R]$ is the multiplier matrix and

$$\{d\} = \left\{u_{,x}^0 + \frac{w}{R_x}\ u_{,y}^0\ v_{,x}^0\ v_{,y}^0 + \frac{w}{R_y}\ w_{,x} - \frac{u}{R_x}\ w_{,y} - \frac{v}{R_y}\ \theta_{x,x}\ \theta_{x,y}\ \theta_{y,x}\ \theta_{y,y}\ \theta_x\ \theta_y\right\}^{\mathrm{T}}. \tag{16}$$

Now, $\{d\}$ can be expressed in the form of nodal degrees of freedom as

$$\{d\} = [G]\{\delta_e\}, \tag{17}$$

where

$$[G] = \sum_{i=1}^{8} \begin{bmatrix} N_{i,x} & 0 & N_i/R_x & 0 & 0 \\ N_{i,y} & 0 & 0 & 0 & 0 \\ 0 & N_{i,x} & 0 & 0 & 0 \\ 0 & N_{i,y} & N_i/R_y & 0 & 0 \\ -N_i/R_x & 0 & N_{i,x} & 0 & 0 \\ 0 & -N_i/R_y & N_{i,y} & 0 & 0 \\ 0 & 0 & 0 & N_{i,x} & 0 \\ 0 & 0 & 0 & N_{i,y} & 0 \\ 0 & 0 & 0 & 0 & N_{i,x} \\ 0 & 0 & 0 & 0 & N_{i,y} \\ 0 & 0 & 0 & N_i & 0 \\ 0 & 0 & 0 & 0 & N_i \end{bmatrix} \tag{18}$$

and $\{\delta_e\} = \{u_1^0\ v_1^0\ w_1\ \theta_{x1}\ \theta_{y1}\ \ldots\ u_8^0\ v_8^0\ w_8\ \theta_{x8}\ \theta_{y8}\}^{\mathrm{T}}$.

The initial stress stiffness matrix is finally expressed in the form [3] of

$$[K_{\sigma e}] = \int_{-1}^{1}\int_{-1}^{1} [G]^{\mathrm{T}}[S][G]\,J\,\mathrm{d}\xi\,\mathrm{d}\eta, \tag{19}$$

where $[S]$ is expressed by

$$[S] = \begin{bmatrix} N_x & & & & & & & & & & & \\ N_{xy} & N_y & & & & & & & & & & \\ 0 & 0 & N_x & & & & & & & & & \\ 0 & 0 & N_{xy} & N_y & & & sym & & & & & \\ 0 & 0 & 0 & 0 & N_x & & & & & & & \\ 0 & 0 & 0 & 0 & N_{xy} & N_y & & & & & & \\ 0 & 0 & -M_x & -M_{xy} & 0 & 0 & \frac{N_x h^2}{12} & & & & & \\ 0 & 0 & -M_{xy} & -M_y & 0 & 0 & \frac{N_{xy}h^2}{12} & \frac{N_y h^2}{12} & & & & \\ M_x & M_{xy} & 0 & 0 & 0 & 0 & 0 & 0 & \frac{N_x h^2}{12} & & & \\ M_{xy} & M_y & 0 & 0 & 0 & 0 & 0 & 0 & \frac{N_{xy}h^2}{12} & \frac{N_y h^2}{12} & & \\ 0 & 0 & -Q_x & -Q_y & 0 & 0 & 0 & 0 & 0 & 0 & 0 & \\ Q_x & Q_y & 0 & 0 & 0 & 0 & 0 & 0 & 0 & 0 & 0 & 0 \end{bmatrix}. \tag{20}$$

The first phase of the solution process is to obtain the initial displacements $\{\delta^i\}$ due to moisture and temperature in static conditions from the equilibrium equation

$$[K]\{\delta^i\} = \{P^N\}, \tag{20}$$

where $\{P^N\}$ is the global load vector due to hygrothermal effects. It leads to get the residual strain values. Then the initial stress resultants are found from equation (5). Consequently, the element initial stress stiffness matrices (equation (19)) are achieved.

2.2. DYNAMIC EQUILIBRIUM EQUATIONS

Neglecting the effects of damping, the assembly of element stiffness matrix, element initial stress stiffness matrix, mass matrix and the load vector leads to the global dynamic equations of equilibrium as

Free vibration

$$[M]\{\ddot{u}\} + \{[K] + [K_\sigma]\}\{u\} = 0. \tag{21}$$

Forced vibration

$$[M]\{\ddot{u}\} + \{[K] + [K_\sigma]\}\{u\} = \{F\}. \tag{22}$$

Here, $\{u\}$ and $\{\ddot{u}\}$ are the global displacement and acceleration vectors, respectively, and $[M]$ is the global mass matrix, $[K]$, the global stiffness matrix, $[K_\sigma]$, the global residual stiffness matrix and $\{F\}$ is the global load vector.

3. MULTIPLE DELAMINATION MODELLING

A typical composite laminate having p number of delaminations is considered as shown in Figure 3. The displacement field within any sublaminate t is denoted by

$$u_t = u_t^0 + (z - z_t^0)\theta_x, \quad v_t = v_t^0 + (z - z_t^0)\theta_y, \tag{23}$$

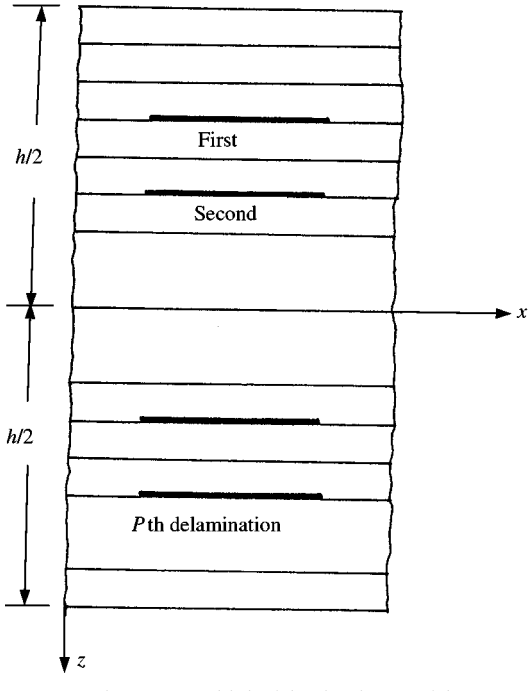

Figure 3. Multiple delamination model.

where u_t^0, v_t^0 are the midplane displacements of the tth sublaminate and z_t^0, the distance between the midplane of the original laminate and the midplane of the tth sublaminate. The strain components at any layer of a sublaminate are found from equation (23) in the form of

$$\begin{Bmatrix} \varepsilon_{xx} \\ \varepsilon_{yy} \\ \gamma_{xy} \end{Bmatrix}_t = \begin{Bmatrix} \varepsilon_{xx}^0 \\ \varepsilon_{yy}^0 \\ \gamma_{xy}^0 \end{Bmatrix}_t + (z - z_t^0) \begin{Bmatrix} k_{xx} \\ k_{yy} \\ k_{xy} \end{Bmatrix}. \tag{24}$$

In order to satisfy the compatibility condition at the delamination boundary, it is assumed that transverse displacements and rotations at a common node for all the three sublaminates including the original one are identical. Applying this multipoint constraint condition, the midplane displacements of any sublaminate t can be generalized as

$$u_t^0 = u^0 + z_t^0 \theta_x, \quad v_t^0 = v^0 + z_t^0 \theta_y. \tag{25}$$

The midplane strain components of the tth sublaminate are derived from it as

$$\begin{Bmatrix} \varepsilon_{xx}^0 \\ \varepsilon_{yy}^0 \\ \gamma_{xy}^0 \end{Bmatrix}_t = \begin{Bmatrix} \varepsilon_{xx}^0 \\ \varepsilon_{yy}^0 \\ \gamma_{xy}^0 \end{Bmatrix} + z_t^0 \begin{Bmatrix} k_{xx} \\ k_{yy} \\ k_{xy} \end{Bmatrix}. \tag{26}$$

Equation (26) is substituted into equation (24) to get the strain components at any layer within a sublaminate. For any lamina of the tth sublaminate, the in-plane and shear stresses are found from the relations

$$\begin{Bmatrix} \sigma_{xx} \\ \sigma_{yy} \\ \tau_{xy} \end{Bmatrix} = \begin{bmatrix} \bar{Q}_{11} & \bar{Q}_{12} & \bar{Q}_{16} \\ \bar{Q}_{12} & \bar{Q}_{22} & \bar{Q}_{26} \\ \bar{Q}_{16} & \bar{Q}_{26} & \bar{Q}_{66} \end{bmatrix} \begin{Bmatrix} \varepsilon_{xx} \\ \varepsilon_{yy} \\ \gamma_{xy} \end{Bmatrix}_t, \tag{27}$$

$$\begin{Bmatrix} \tau_{xz} \\ \tau_{yz} \end{Bmatrix} = \begin{bmatrix} \bar{Q}_{44} & \bar{Q}_{45} \\ \bar{Q}_{45} & \bar{Q}_{55} \end{bmatrix} \begin{Bmatrix} \gamma_{xz} \\ \gamma_{yz} \end{Bmatrix}_t. \tag{28}$$

Integrating these stresses over the thickness of the sublaminate, the stress and moment resultants of the sublaminate are derived which lead to the elasticity matrix of the tth sublaminate in the form

$$[D]_t = \begin{bmatrix} A_{ij} & z_t^0 A_{ij} + B_{ij} & 0 \\ B_{ij} & z_t^0 B_{ij} + D_{ij} & 0 \\ 0 & 0 & S_{ij} \end{bmatrix}, \tag{29}$$

where

$$[A_{ij}]_t = \int_{-h_t/2 + z_t^0}^{h_t/2 + z_t^0} [\bar{Q}_{ij}]\, \mathrm{d}z, \quad [B_{ij}]_t = \int_{-h_t/2 + z_t^0}^{h_t/2 + z_t^0} [\bar{Q}_{ij}](z - z_t^0)\, \mathrm{d}z,$$

$$[D_{ij}]_t = \int_{-h_t/2 + z_t^0}^{h_t/2 + z_t^0} [\bar{Q}_{ij}](z - z_t^0)^2\, \mathrm{d}z, \quad i,j = 1,2,6, \quad [S_{ij}]_t = \int_{-h_t/2 + z_t^0}^{h_t/2 + z_t^0} [\bar{Q}_{ij}]\, \mathrm{d}z, \quad i,j = 4,5.$$

Here, h_t is the thickness of the tth sublaminate.

4. NUMERICAL RESULTS AND DISCUSSION

Based on the above finite element hygrothermal analysis and multiple delamination modelling, computer codes are developed to generate numerical results for studying the free vibration and transient response of delaminated doubly curved composite shells exposed to moisture and temperature. The formulation can handle any general distribution of moisture and temperature in addition to the external loads. The accuracy of the present finite element formulation is verified by comparing it with the non-dimensional frequency results of Sai Ram and Sinha [3] and Ritz method [1] as shown in Table 1. The material properties are assumed to be constant irrespective of moisture and temperature absorption for this case.

For the present dynamic analysis in the hygrothermal environment, moisture concentration is varied from 0 to 1·5% and temperature from 300 to 425 K. For computing the results, centrally located single and multiple delaminations are considered for various doubly curved shells. Single midplane delamination of two different sizes like 25 and 56·25% of the total plate area are considered. Three different types of delaminations like (1) single midplane delamination (2) three uniform delaminations and (3) five uniform delaminations are analyzed. For case (2), delamination interfaces are located after 8th, 10th and 12th ply and for case (3), delaminations are considered after 6th, 8th, 10th, 12th and 14th ply. For all the laminates considered below for free and forced vibration analysis, the simply supported boundary condition is adopted.

The mechanical properties for the carbon-epoxy composites and the shell planform geometry are assumed to be as follows:

$E_1 = 172{\cdot}5$ GPa, $E_2 = E_3 = 6{\cdot}9$ GPa, $G_{12} = G_{13} = 3{\cdot}45$ GPa, $G_{23} = 1{\cdot}38$ GPa, $\rho = 1600$ kg/m^3, $v_{12} = 0{\cdot}25$, $a = b = 0{\cdot}5$ m, $h = 5$ mm, $a/h = 100$.

TABLE 1

Non-dimensional frequency $\lambda = [\omega_n a^2(\rho/E_2h^2)^{1/2}]$ *of simply supported* (0/90/90/0) *plate*, $a/b = 1$, $a/h = 100$

Mode number m	$C = 0{\cdot}1\%$			$T = 325$ K		
	Sai Ram and Sinha [3]	Present FEM	Ritz method [1]	Sai Ram and Sinha [3]	Present FEM	Ritz method [1]
1	9·429	9·393	9·411	8·088	8·046	8·068
2	20·679	19·887	19·911	19·196	18·350	18·378
3	40·068	39·345	39·528	39·324	38·590	38·778

TABLE 2

Elastic moduli of carbon-epoxy lamina at different moisture concentrations; $G_{13} = G_{12}$, $G_{23} = 0{\cdot}4G_{12}$, $\beta_1 = 0$, $\beta_2 = 0{\cdot}44$

Elastic moduli (GPa)	Moisture concentration, C (%)						
	0·00	0·25	0·50	0·75	1·00	1·25	1·50
E_1	172·5	172·5	172·5	172·5	172·5	172·5	172·5
E_2	6·9	6·72	6·54	6·36	6·17	6·17	6·17
G_{12}	3·45	3·45	3·45	3·45	3·45	3·45	3·45

The lamina material properties at the elevated moisture concentrations and temperatures used in the present analysis are shown in Tables 2 and 3 respectively. Numerical convergence of results for the present dynamic analysis is carried out testing with various mesh sizes of the laminates as well the timesteps. The converged mesh size and timestep used in the analysis are 8×8 and 10 μs respectively.

4.1. FREE VIBRATION

In the present investigation, the results are presented for antisymmetric delaminated crossply and angleply laminates subjected to uniform distribution of moisture and

TABLE 3

Elastic moduli of carbon-epoxy lamina at different temperatures; $G_{13} = G_{12}$, $G_{23} = 0{\cdot}4G_{12}$, $\alpha_1 = -0{\cdot}3 \times 10^{-6}$/K, $\alpha_2 = 28{\cdot}1 \times 10^{-6}$/K

Elastic moduli (GPa)	Temperature T (K)					
	300	325	350	375	400	425
E_1	172·5	172·5	172·5	172·5	172·5	172·5
E_2	6·9	6·17	5·81	5·45	5·08	4·9
G_{12}	3·45	3·45	3·16	2·88	2·73	2·59

TABLE 4

Variation of first natural frequency, f_1 (Hz) for midplane delaminated spherical shells ($R_x = R_y = R$, $R_{xy} = \infty$) and plates for different moisture contents

Delamination size	Stacking sequence	$C = 0$	$C = 0{\cdot}25\%$	$C = 0{\cdot}5\%$	$C = 0{\cdot}75\%$	$C = 1\%$	$C = 1{\cdot}5\%$
		$R/a = 5$					
No delamination	$(0/90)_2$	202·02	201·91	201·82	201·72	201·64	201·44
	$(45/-45)_2$	347·52	346·35	345·23	344·18	343·18	340·97
25%	$(0/90)_2$	187·51	187·40	187·30	187·21	187·12	186·93
	$(45/-45)_2$	292·23	291·73	291·24	290·77	290·32	289·29
56·25%	$(0/90)_2$	183·96	183·78	183·61	183·45	183·29	182·95
	$(45/-45)_2$	264·73	276·82	287·54	297·08	292·13	—
		$R/a = 10$					
No delamination	$(0/90)_2$	129·20	128·96	128·73	128·52	128·32	127·87
	$(45/-45)_2$	301·13	297·03	293·09	289·32	285·75	277·70
25%	$(0/90)_2$	104·59	104·40	104·22	104·05	103·89	103·55
	$(45/-45)_2$	225·10	222·26	219·51	216·85	214·33	208·58
56·25%	$(0/90)_2$	98·36	98·03	97·72	97·42	97·14	96·51
	$(45/-45)_2$	182·98	180·28	177·63	175·04	172·53	166·69
		$R/a = \infty$ (plate)					
No delamination	$(0/90)_2$	92·72	92·16	91·63	91·13	90·65	89·60
	$(45/-45)_2$	124·26	98·23	64·58	—	—	—
25%	$(0/90)_2$	52·93	51·91	50·92	49·96	49·05	46·99
	$(45/-45)_2$	90·82	44·33	—	—	—	—
56·25%	$(0/90)_2$	39·50	38·14	36·80	35·48	34·20	31·16
	$(45/-45)_2$	71·16	—	—	—	—	—

temperature. Fundamental natural frequencies, f_1 (Hz) for various spherical shells are presented in Tables 4 and 5 with different sizes of central midplane delaminations subjected to the effect of moisture content and temperature respectively. Three different R/a ratios are considered. It is obvious from the tables that with an increase in R/a ratio, the natural frequency decreases. The increase in percentage of moisture content as well as temperature reduces the natural frequencies. It is caused due to the reduction in the value of residual stiffness matrix with increase in moisture content/temperature which finally reduces the global stiffness. Again, with an increase in the size of delamination, the natural frequency decreases due to the overall reduction in stiffness of the laminate. The f_1 value is observed to be lower for crossply laminate for all the cases considered. Results for cylindrical shells for similar cases are shown in Tables 6 and 7 for moisture and temperature respectively. As observed, the effect of delamination is more predominant in the case of a cylindrical shell compared to a spherical shell. Table 8 presents the effect of multiple delamination for two different laminates for varying percentages of moisture content. The temperature effect for the similar cases is shown in Table 9. Tables 4 and 5 depict that, the equilibrium of midplane delaminated $(45/-45)_2$ plate becomes unstable at higher moisture contents and temperatures, which does not occur for crossply laminates. A similar observation is also revealed for multiple delaminated $(45/-45)_{10}$ plate presented in Tables 8 and 9. The instability seems to be a function of both hygrothermal effect as well as the magnitude of the delamination.

TABLE 5

Variation of first natural frequency, f_1 (Hz) for midplane delaminated spherical shells ($R_x = R_y = R$, $R_{xy} = \infty$) and plates for different temperatures (K)

Delamination size	Stacking sequence	$T = 300$	$T = 325$	$T = 350$	$T = 375$	$T = 400$	$T = 425$
				$R/a = 5$			
No delamination	$(0/90)_2$	202·02	201·96	201·91	201·87	201·84	201·84
	$(45/-45)_2$	347·52	347·00	346·56	346·19	345·91	345·61
25%	$(0/90)_2$	187·51	187·44	187·39	187·34	187·30	187·25
	$(45/-45)_2$	292·23	292·01	291·81	291·65	291·53	291·40
56·25%	$(0/90)_2$	183·96	183·85	183·76	183·67	183·60	183·53
	$(45/-45)_2$	259·43	259·17	258·94	258·75	258·61	258·45
				$R/a = 10$			
No delamination	$(0/90)_2$	129·20	129·08	128·99	128·90	128·84	128·77
	$(45/-45)_2$	301·13	299·31	297·77	296·49	295·51	294·44
25%	$(0/90)_2$	104·59	104·48	104·39	104·32	104·25	104·18
	$(45/-45)_2$	225·10	223·84	222·76	221·88	221·19	220·44
56·25%	$(0/90)_2$	98·36	98·17	98·00	97·86	97·73	97·60
	$(45/-45)_2$	182·98	181·79	180·77	179·92	179·26	178·54
				$R/a = \infty$ (plate)			
No delamination	$(0/90)_2$	92·72	92·47	92·26	92·09	91·96	91·82
	$(45/-45)_2$	124·26	113·42	103·36	94·32	86·77	77·76
25%	$(0/90)_2$	52·93	52·48	52·09	51·78	51·54	51·27
	$(45/-45)_2$	90·82	74·12	55·80	33·40	—	—
56·25%	$(0/90)_2$	39·50	38·91	38·39	37·97	37·64	37·28
	$(45/-45)_2$	71·16	46·89	—	—	—	—

TABLE 6

Variation of first natural frequency, f_1 (Hz) for midplane delaminated cylindrical shells ($R_x = \infty$, $R_{xy} = \infty$) for different moisture contents

Delamination size	Stacking sequence	$C = 0$	$C = 0{\cdot}25\%$	$C = 0{\cdot}5\%$	$C = 0{\cdot}75\%$	$C = 1\%$	$C = 1{\cdot}5\%$
				$R_y/a = 5$			
No delamination	$(0/90)_2$	129·04	128·83	128·64	128·45	128·28	127·90
	$(45/-45)_2$	294·93	290·50	286·23	282·14	278·26	269·50
25%	$(0/90)_2$	104·56	104·41	104·27	104·14	104·02	103·75
	$(45/-45)_2$	216·73	213·06	209·51	206·09	202·83	195·42
56·25%	$(0/90)_2$	98·24	97·98	97·74	97·50	97·27	96·76
	$(45/-45)_2$	173·07	169·24	165·50	161·86	158·35	150·23
				$R_y/a = 10$			
No delamination	$(0/90)_2$	103·03	102·62	102·24	101·87	101·53	100·77
	$(45/-45)_2$	193·38	186·32	179·38	172·58	165·98	150·40
25%	$(0/90)_2$	69·60	69·14	68·71	68·29	67·90	67·04
	$(45/-45)_2$	168·02	161·58	155·19	148·87	142·65	107·61
56·25%	$(0/90)_2$	59·88	59·33	58·76	58·22	57·70	56·53
	$(45/-45)_2$	153·51	143·03	131·27	119·07	101·98	30·12

TABLE 7

Variation of first natural frequency, f_1 (Hz) for midplane delaminated cylindrical shells ($R_x = \infty$, $R_{xy} = \infty$) for different temperatures (K)

Delamination size	Stacking sequence	$T = 300$	$T = 325$	$T = 350$	$T = 375$	$T = 400$	$T = 425$
				$R_y/a = 5$			
No delamination	$(0/90)_2$	129·04	128·95	128·87	128·81	128·76	128·71
	$(45/-45)_2$	294·93	292·97	291·29	289·91	288·85	287·70
25%	$(0/90)_2$	104·56	104·48	104·42	104·37	104·32	104·28
	$(45/-45)_2$	216·73	215·11	213·72	212·57	211·69	210·73
56·25%	$(0/90)_2$	98·24	98·11	97·98	97·88	97·80	97·70
	$(45/-45)_2$	173·07	171·38	169·93	168·73	167·80	166·79
				$R_y/a = 10$			
No delamination	$(0/90)_2$	103·03	102·85	102·70	102·57	102·48	102·37
	$(45/-45)_2$	193·38	190·27	187·60	185·38	183·66	181·78
25%	$(0/90)_2$	69·60	69·39	69·21	69·05	68·93	68·80
	$(45/-45)_2$	168·02	165·19	162·75	160·72	159·14	157·41
56·25%	$(0/90)_2$	59·88	59·63	59·37	59·15	58·97	58·78
	$(45/-45)_2$	153·51	149·47	145·13	141·47	138·59	135·41

4.2. TRANSIENT RESPONSE

Transient response for single and multiple delaminated plates and shells subjected to hygrothermal environment is computed applying Newmark's constant average acceleration method [15]. A uniform transverse pulse load of 100 N/m^2 is considered in the analysis for

TABLE 8

First natural frequencies, f_1 (Hz) for different laminates with centrally located multiple delaminations of 25% showing the moisture effect

Multiple delaminations	Plate							
	$(0/90)_{10}$ Moisture percentage (C)				$(45/-45)_{10}$ Moisture percentage (C)			
	0%	0·5%	1%	1·5%	0%	0·5%	1%	1·5%
One	66·63	62·79	59·17	55·06	107·98	31·40	—	—
Three	57·77	53·29	48·97	43·90	99·94	—	—	—
Five	51·23	46·10	40·99	34·75	92·13	—	—	—
	Cylindrical shell ($R_y/a = 5$)							
One	112·03	111·76	111·52	111·26	258·20	250·29	243·03	235·05
Three	107·10	107·07	107·03	106·99	235·04	227·33	220·23	212·37
Five	103·83	103·76	103·60	103·35	213·67	206·06	198·99	191·12
	Spherical shell ($R/a = 5$)							
One	191·70	191·66	191·62	191·57	322·15	320·65	319·27	317·78
Three	188·92	188·63	188·39	188·11	306·28	305·12	304·05	302·88
Five	187·15	186·92	186·74	186·53	293·23	292·38	291·57	290·65

TABLE 9

First natural frequencies, f_1 (Hz) for different laminates with centrally located multiple delaminations of 25% showing the temperature effect

Multiple delaminations	Plate							
	$(0/90)_{10}$ Temperature T(K)				$(45/-45)_{10}$ Temperature, T(K)			
	$T = 300$	$T = 350$	$T = 400$	$T = 425$	$T = 300$	$T = 350$	$T = 400$	$T = 425$
One	66·63	65·03	63·96	63·44	107·98	82·28	59·24	44·37
Three	57·77	55·93	54·67	54·06	99·94	70·11	38·16	—
Five	51·23	49·13	47·68	46·99	92·13	51·00	—	—
	Cylindrical shell ($R_y/a = 5$)							
One	112·03	111·91	111·83	111·80	258·20	254·89	252·67	251·62
Three	107·10	107·09	107·07	107·03	235·04	231·82	229·66	228·63
Five	103·83	103·80	103·76	103·67	213·67	210·50	208·36	207·35
	Spherical shell ($R/a = 5$)							
One	191·70	191·68	191·66	191·65	322·15	321·52	321·10	320·90
Three	188·92	188·87	188·81	188·72	306·28	305·80	305·47	305·32
Five	187·15	187·12	187·06	186·98	293·23	292·88	292·64	292·52

all the cases. Figure 4 shows the central dynamic displacement for a $(0/90)_{10}$ plate for different sizes of single midplane delaminations. The plot depicts an increase in dynamic displacement with an increase in moisture content for any delamination size considered. Plots for central displacement versus time for the same laminate are presented in Figure 5 to

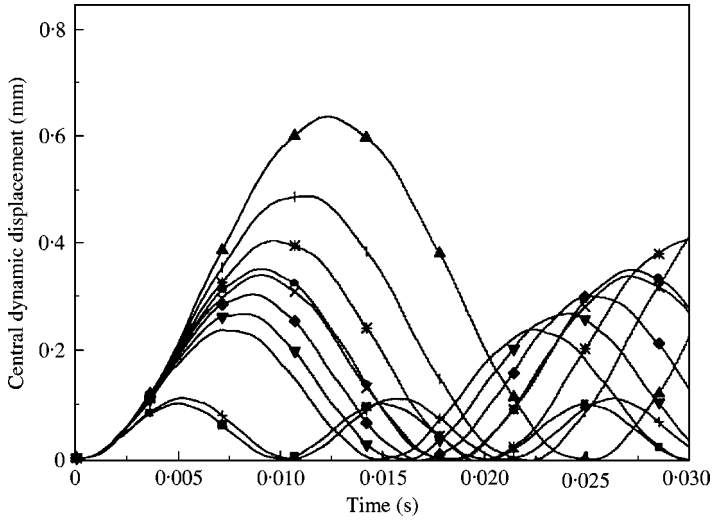

Figure 4. Effect of moisture on the transient response of a central midplane delaminated $(0/90)_{10}$ plate: —■—, case 1, $C = 0$; —+—, case 1, $C = 1\%$; ——, case 2, $C = 0$; —▼—, case 2, $C = 0{\cdot}5\%$; —♦—, case 2, $C = 1\%$; —●—, case 2, $C = 1{\cdot}5\%$; —×—, case 3, $C = 0$; —✲—, case 3, $C = 0{\cdot}5\%$; —+—, case 3, $C = 1\%$; —▲—, case 3, $C = 1{\cdot}5\%$: case 1 (no delamination), case 2 (25% delamination) and case 3 (56·25% delamination).

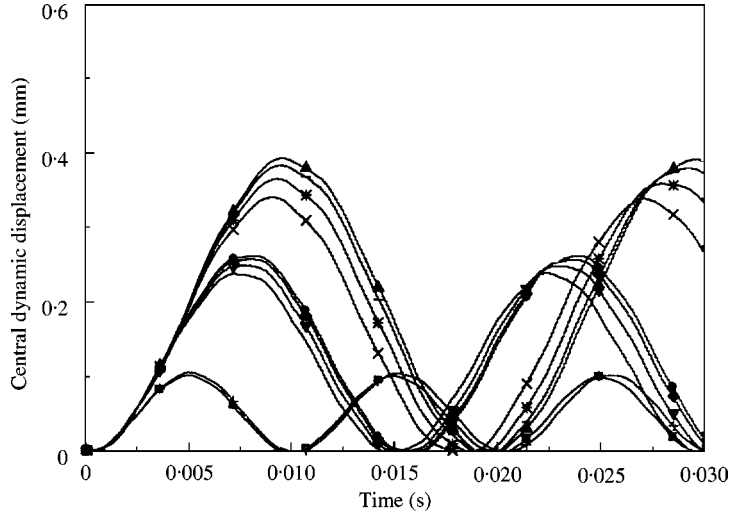

Figure 5. Effect of temperature on the transient response of a central midplane delaminated $(0/90)_{10}$ plate: —■—, case 1, $T = 300$ K; —+—, case 1, $T = 400$ K; ——, case 2, $T = 300$ K; —▼—, case 2, $T = 350$ K; —♦—, case 2, $T = 400$ K; —●—, case 2, $T = 425$ K; —×—, case 3, $T = 300$ K; —✲—, case 3, $T = 350$ K; ——, case 3, $T = 400$ K; —▲—, case 3, $T = 425$ K: case 1 (no delamination), case 2 (25% delamination) and case 3 (56·25% delamination).

show the effect of temperature. The moisture and the temperature effects on the same crossply laminate with increasing number of delaminations (each delamination interface of 25%) are presented in Figures 6 and 7 respectively. For a multiple delaminated spherical shell ($R/a = 5$), the transient responses are depicted in Figures 8 and 9 considering moisture and temperature effects respectively. Compared to the plates, the effects of moisture and temperature on the transient response of shells seem to be negligible. A cylindrical shell ($R_y/a = 5$) with multiple delaminations is considered in Figure 10 to observe the effect of

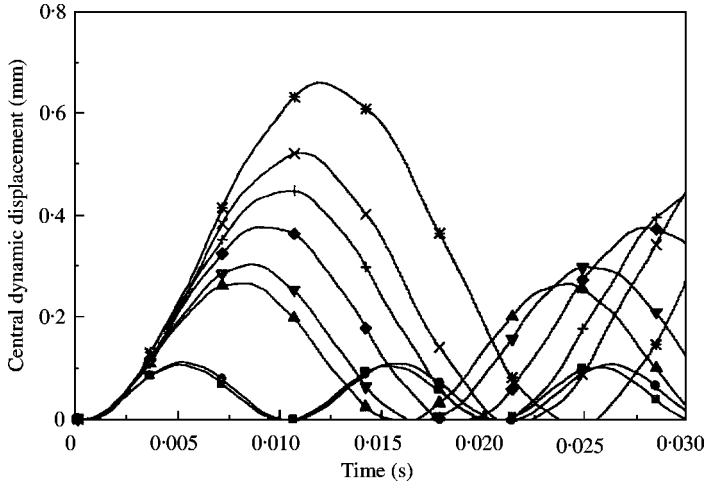

Figure 6. Effect of moiture on the transient response of multiple delaminated $(0/90)_{10}$ plate: —■—, w, $C = 0{\cdot}5\%$; —●—, w, $C = 1\%$; —▲—, x, $C = 0{\cdot}5\%$; —▼—, y, $C = 1\%$; —♦—, y, $C = 0{\cdot}5\%$; —+—, y, $C = 1\%$; —×—, z, $C = 0{\cdot}5\%$; —✳—, z, $C = 1\%$: w = no delamination, x = single delamination, y = three delaminations and z = five delaminations.

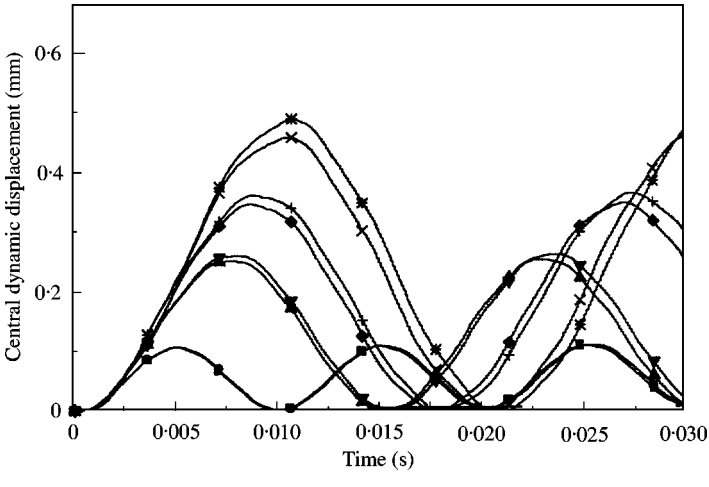

Figure 7. Effect of temperature on the transient response of multiple delaminated $(0/90)_{10}$ plate: —■—, w, $T = 350\,\text{K}$; —●—, w, $T = 400\,\text{K}$; —▲—, x, $T = 350\,\text{K}$; —▼—, x, $T = 400\,\text{K}$; —♦—, y, $T = 350\,\text{K}$; —+—, y, $T = 400\,\text{K}$; —×—, z, $T = 350\,\text{K}$; —✳—, z, $T = 400\,\text{K}$: w = no delamination, x = single delamination, y = three delaminations and z = five delaminations.

moisture concentration. Figure 11 distinguishes the transient responses for plate, spherical and cylindrical shell subjected to the environment of moisture. As shown in the plot, the variation of response with change in moisture content is very negligible in the case of shells. Figure 12 provides the plots for central dynamic normal stress (the top layer), $-\sigma_x$ (MPa) with variation with respect to time for a crossply plate with various increasing midplane delaminations. It exhibits a relatively small increase in the normal stress with increase in moisture content for the no-delamination case and a sharp increase in normal stress for bigger size delaminations. The effect of multiple delaminations on the normal stress (top layer), $-\sigma_x$ (MPa) is depicted in Figure 13 for the same laminate considering two different

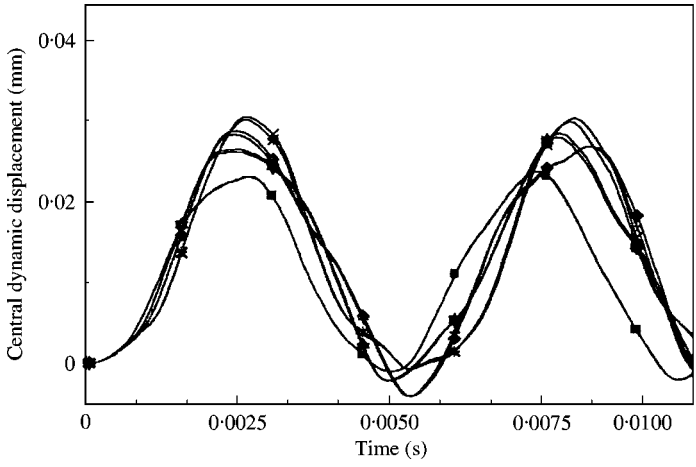

Figure 8. Effect of moisture on the transient response of a multiple delaminated $(0/90)_{10}$ spherical shell ($R/a = 5$): —■—, w, $C = 0$; —●—, w, $C = 1{\cdot}5\%$; —▲—, x, $C = 0$; —▼—, x, $C = 1{\cdot}5\%$; —◆—, y, $C = 0$; —+—, y, $C = 1{\cdot}5\%$; —×—, z, $C = 0$; —✳—, z, $C = 1{\cdot}5\%$: w = no delamination, x = single delamination, y = three delaminations and z = five delaminations.

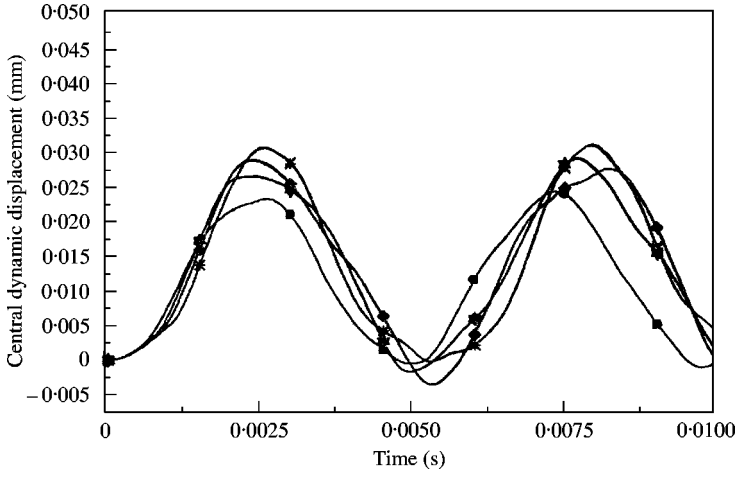

Figure 9. Effect of temperature on the transient response of multiple delaminated $(0/90)_{10}$ spherical shell ($R/a = 5$): —■—, w, $T = 300\,\text{K}$; —●—, w, $T = 425\,\text{K}$; —▲—, x, $T = 300\,\text{K}$; —▼—, x, $T = 425\,\text{K}$; —◆—, y, $T = 300\,\text{K}$; —+—, y, $T = 425\,\text{K}$; —×—, z, $T = 300\,\text{K}$; —✳—, z, $T = 425\,\text{K}$: w = no delamination, x = single delamination, y = three delaminations and z = five delaminations.

percentages of moisture content. In this case, the delamination area in each interface is same as considered earlier.

5. CONCLUSION

A dynamic analysis of multiple delaminated doubly curved composite shells exposed to hygrothermal environment is investigated taking into account the changes in thermomechanical properties due to moisture and temperature effect. The conventional finite element formulation is modified to include the hygrothermal effects. The shell

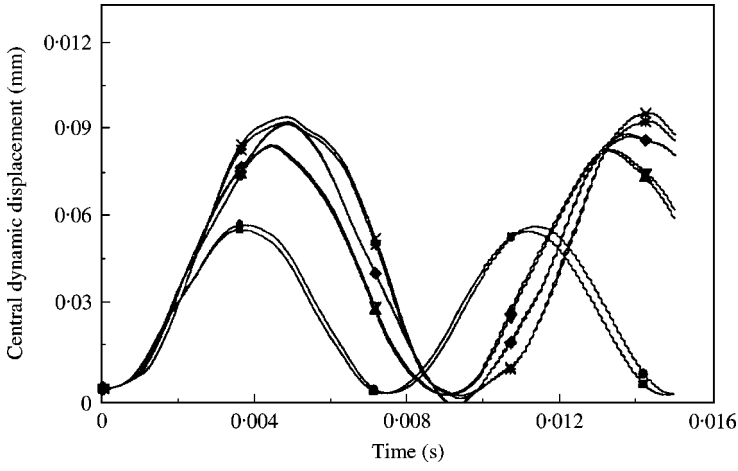

Figure 10. Effect of moisture on the transient response of a multiple delaminated $(0/90)_{10}$ cylindrical shell ($R/a = 5$): —■—, w, $C = 0$; —●—, w, $C = 1{\cdot}5\%$; —▲—, x, $C = 0$; —▼—, x, $C = 1{\cdot}5\%$; —◆—, y, $C = 0$; —+—, y, $C = 1{\cdot}5\%$; —×—, z, $C = 0$; —✳—, z, $C = 1{\cdot}5\%$: w = no delamination, x = single delamination, y = three delaminations and z = five delaminations.

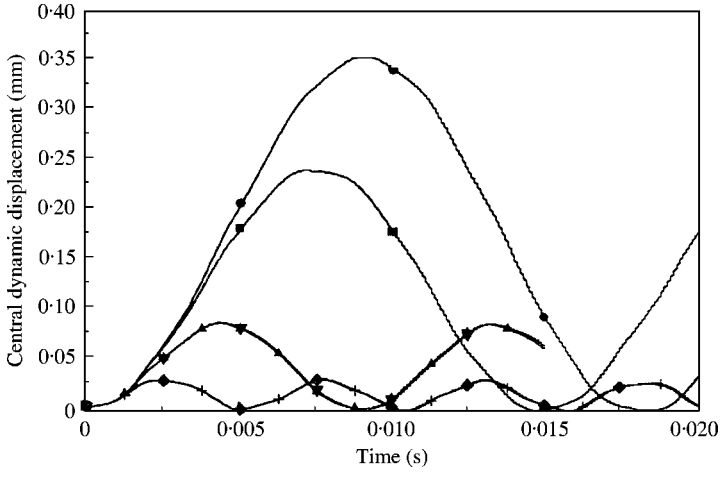

Figure 11. Comparison of dynamic displacement for $(0/90)_{10}$ laminated plate and shells for a single midplane delamination of 25%. —■—, plate, $C = 0$; —●—, plate, $C = 1{\cdot}5\%$; —▲—, cyl. shell, $C = 0$; —▼—, cyl. shell, $C = 1{\cdot}5\%$; —◆—, sph. cell, $C = 0$; —+—, sph. cell, $C = 1{\cdot}5\%$.

strain–deformation relations are based on Sanders' shallow shell theory. The accuracy of the formulation has been verified using sample problems available in the literature. The degradation in the natural frequencies and the increase in the amplitude of dynamic displacements and stresses are influenced by the degree of moisture concentration, temperature variation and also the stacking sequences of the laminate. The reduction in the fundamental frequency need not be linear and the problem may become instable, depending on the values of moisture concentration and temperature. The analysis of numerical results indicate that, there is a greater influence of curvature ratio (R/a) on the values of natural frequencies as well as dynamic displacements.

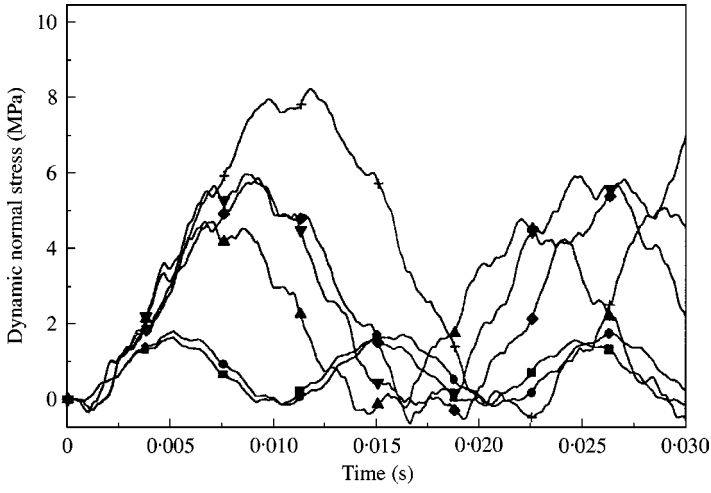

Figure 12. Effect of moisture on the top layer normal stress at the center ($-\sigma_x$) of a midplane delaminated $(0/90)_{10}$ plate due to uniform pulse load. —■—, case 1, $C = 0$; —●—, case 1, $C = 1\%$; —▲—, case 2, $C = 0$; —▼—, case 2, $C = 1\%$; —◆—, case 3, $C = 0$; —+—, case 3, $C = 1\%$: case 1 (no delamination), case 2 (25% delamination) and case 3 (56·25% delamination).

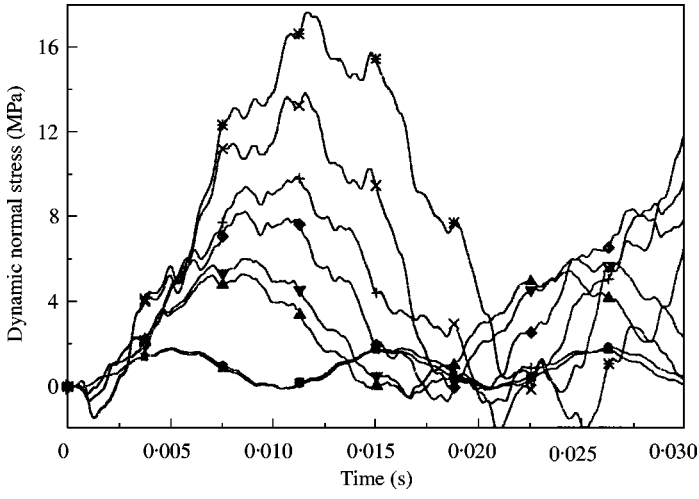

Figure 13. Effect of moisture on the top layer normal stress at the center ($-\sigma_x$) of a multiple delaminated $(0/90)_{10}$ plate due to uniform pulse load. —■—, w, $C = 0{\cdot}5\%$; —●—, w, $C = 1\%$; —▲—, x, $C = 0{\cdot}5\%$; —▼—, x, $C = 1\%$; —◆—, y, $C = 0{\cdot}5\%$; —+—, y, $C = 1\%$; —×—, z, $C = 0{\cdot}5\%$; —✳—, z, $C = 1\%$: w = no delamination, x = single delamination, y = three delaminations and z = five delaminations.

REFERENCES

1. J. M. WHITNEY and J. E. ASHTON 1971 *American Institute of Aeronautics and Astronautics Journal* **9**, 1708–1713. Effect of environment on the elastic response of layered composite plates.
2. R. D. DHANARAJ and PALANINATHAN 1989 *Proceedings of the Seminar on Science and Technology of Composites, Adhesives and Sealants, Bangalore, India*, 245–251. Free vibrational characteristics of composite laminates under initial stress.
3. K. S. SAI RAM and P. K. SINHA 1992 *Journal of Sound and Vibration* **158**, 133–148. Hygrothermal effects on the free vibration of laminated composite plates.
4. J. J. TRACY and G. C. PARDOEN 1989 *Journal of Composite Materials* **23**, 1200–1215. Effect of delamination on the natural frequencies of composite laminates.

5. A. PAOLOZZI and I. PERONI 1992 *Journal of Reinforced Plastics and Composites* **9**, 369–389. Detection of debonding damage in a composite plate through natural frequency variations.
6. M. H. H. SHEN and J. E. GRADY 1992 *American Institute of Aeronautics and Astronautics Journal* **30**, 1361–1370. Free vibrations of delaminated beams.
7. L. H. TENEK, E. G. HENNEKELL and M. D. GUNZBURGER 1993 *Composite Structures* **23**, 253–262. Vibration of delaminated composite plates and some applications to non-destructive testing.
8. M. KRAWCZUK, W. OSTACHOWICZ and A. ZAK 1997 *Computational Mechanics* **20**, 79–83. Dynamics of cracked composite material structures.
9. P. K. PARHI, S. K. BHATTACHARYYA and P. K. SINHA 2000 *Journal of Reinforced Plastics and Composites* **19**, 863–882. Finite element dynamic analysis of laminated composite plates with multiple delaminations.
10. P. K. PARHI, S. K. BHATTACHARYYA and P. K. SINHA 1999 *Aircraft Engineering and Aerospace Technology*, *an International Journal* **71**, 451–461. Dynamic analysis of multiple delaminated composite twisted plates.
11. P. K. PARHI, S. K. BHATTACHARYYA and P. K SINHA 2000 *International Journal of Crashworthiness* **5**, 63–77. Failure analysis of multiple delaminated composite plates due to low velocity impact.
12. P. K. PARHI, S. K. BHATTACHARYYA and P. K. SINHA 2000 *Journal of Reinforced Plastics and Composites*. Dynamic behavior and impact induced first ply failure of multiple delaminated composite shells (in press).
13. R. D. COOK, D. S. MALKUS and M. E. PLESHA 1989 *Concepts and Applications of Finite Element Analysis*. New York: John Wiley and Sons.
14. S. Y. LEE and W. J. YEN 1989 *Computers and Structures* **33**, 551–559. Hygrothermal effects on the stability of a cylindrical composite shell panel.
15. K. J. BATHE 1982 *Finite Element Procedures in Engineering Analysis*. Englewood Cliffs, NJ: Prentice-Hall.